Contents lists available at ScienceDirect

Arabian Journal of Chemistry

journal homepage: www.ksu.edu.sa

Fast thermo-responsive thermoset self-healing polymers based on bio-derived Benzoxazine/Epoxidized castor oil copolymers for coating applications

Phattarin Mora [a], Sarawut Rimdusit [b], Chanchira Jubsilp [a,*]

[a] Department of Chemical Engineering, Faculty of Engineering, Srinakharinwirot University, Nakhonnayok 26120, Thailand
[b] Center of Excellence in Polymeric Materials for Medical Practice Devices, Department of Chemical Engineering, Faculty of Engineering, Chulalongkorn University, Bangkok 10330, Thailand

ARTICLE INFO

Keywords:
Self-healing polymer
Polybenzoxazine
Epoxidized castor oil
Bio-derived polymer
Numerical simulation

ABSTRACT

This work emphasized on development of a novel bio-derived self-healing copolymer fabricated from benzoxazine and epoxy resins by varying weight ratios. The bio-derived benzoxazine (E-fa) acted as a healing agent was copolymerized with bio-derived epoxy resin namely epoxidized castor oil (ECO). Three main essential properties of the developed copolymer were systematically investigated: thermal property, mechanical property, and self-healing capacity. The numerical simulation was also used to study and predict the ability of roof coatings based on the developed copolymers. The results showed that the reversible crosslinking reaction occurred and resulted in state transition of the copolymers. The mechanical property i.e., tensile strength and peel strength to stainless steel substrate, were substantially improved with the incorporation of ECO. The increase in E-fa contents can enhance the thermos-responsive healing performance of the copolymers up to 93% via reversible reactions with rapid surface damage healed within 2 min. Furthermore, the experimental and numerical results revealed that the thermo-responsive thermoset self-healing bio-derived benzoxazine/epoxy copolymers have a potential use in coating applications required fast self-healing performance and good mechanical properties.

1. Introduction

Self-healing polymers (SHPs) are smart polymers which can autonomic or externally repair their damage triggered by various stimuli, such as heat (Imato et al., 2012; Mora et al., 2023), light (Ji et al., 2015; Leungpuangkaew et al., 2023; Zhao et al., 2024), solvent (Huang et al., 2005) and stress (Wu et al., 2021). The application fields of SHPs are diverse smart medical devices, aerospace, 4D Printing, sensor, especially coatings with intelligence (Liu et al., 2018; Mrlík et al., 2020; Ying et al., 2020). Self-healing materials are classified into two groups by healing mechanism: extrinsic and intrinsic self-healing (Rahman & Shefa, 2021). The introduction of exogenous chemicals initiates extrinsic SHPs, which then facilitates self-healing from implanted microcapsules upon breaking (An et al., 2018). Whereas, intrinsic type self-healing can repair damage by momentarily enhancing the polymeric chains mobility (Urban, 2014). In recent years, significant researches have extensively explored the potential for developing materials with the self-healing ability in order to prolong their overall life-cycle and to heal micron-sized cracks and damage with the least amount of outside assistance (Amaral & Pasparakis, 2017; Arslan et al., 2018a; Arslan et al., 2018b; Fadl et al., 2021). One of the effective strategies for self-healing polymers is from covalent bonds reforming that led to high self-healing capacity (Amornkitbamrung et al., 2022; Chao et al., 2016; Xu et al., 2021a; Yang & Urban, 2013).

Polybenzoxazines are commonly recognized as a thermoset polymer that is constantly being researched, particularly for use in thermosetting smart materials. The thermal curing of polybenzoxazine generally provides a highly helpful function group—phenolic moiety—permits further reaction with other resins or polymers (Ishida & Agag, 2011; Rimdusit et al., 2013). The intriguing features of smart materials systems especially self-healing polymers from the incorporation of polybenzoxazine have attracted the interest of numerous researchers. Investigations on self-healing polymers utilizing the polybenzoxazine hybrid system have been published, including polybenzoxazine/polysulfones (Oie et al., 2013), polybenzoxazine/ poly(propylene oxide) bisamine (Arslan et al., 2015), and polybenzoxazine/epoxy

* Corresponding author.
E-mail address: chanchira@g.swu.ac.th (C. Jubsilp).

https://doi.org/10.1016/j.arabjc.2024.106005
Received 9 May 2024; Accepted 18 September 2024
Available online 21 September 2024

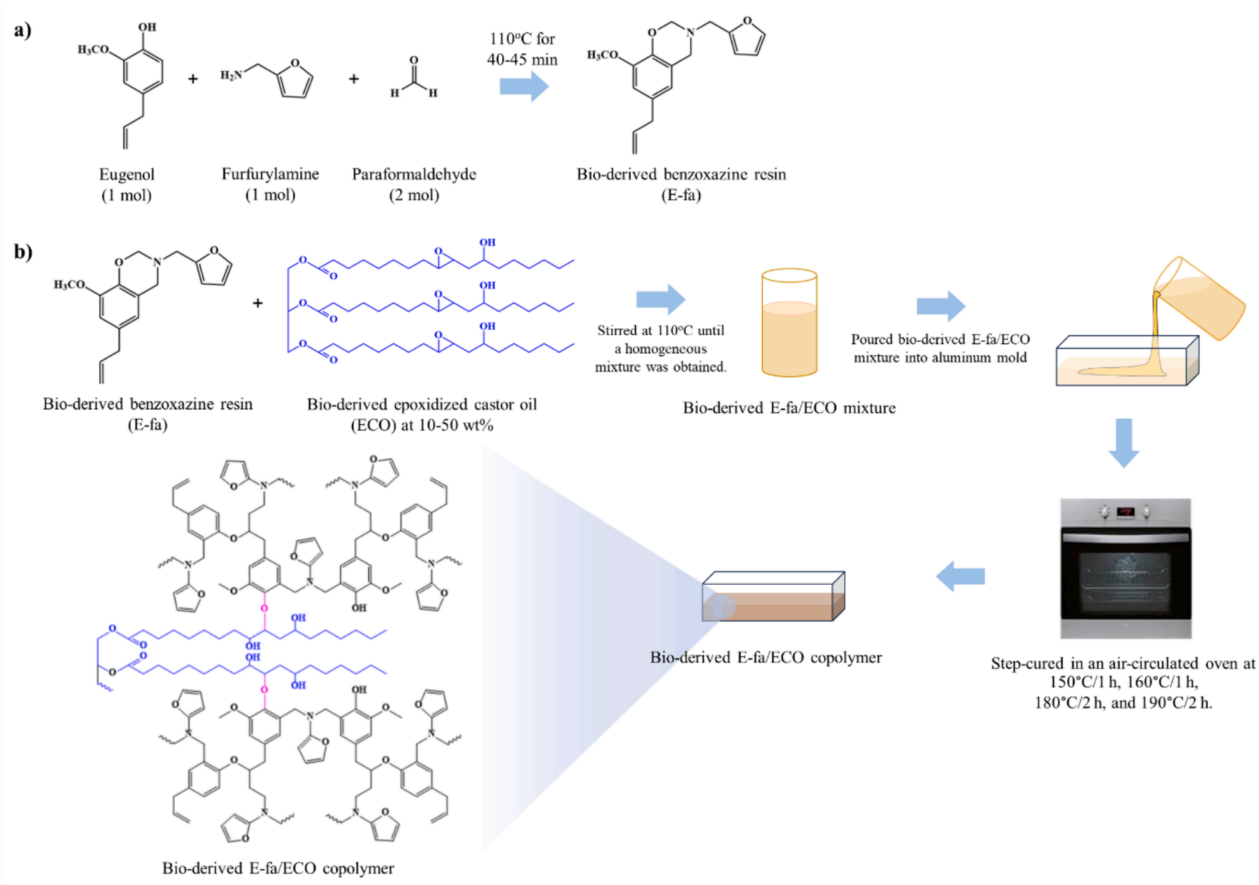

Scheme 1. Preparation of a) bio-derived benzoxazine resin and b) bio-derived benzoxazine/epoxy copolymer.

(Amornkitbamrung et al., 2022). However, benzoxazine resin is broadly synthesized from basic chemicals found in petroleum resources for the previous works. Therefore, with the global environmental issues and growing energy crisis, exploration on using renewable substances to create bio-derived benzoxazine resin has become increasingly focused including intelligent polymeric materials (Hombunma et al., 2019; Prasomsin et al., 2019).

In term of stimuli for self-healing, heating is gain wider attention because of its advantages of convenient processing, general activation, and precise control (Fang et al., 2017; Gao et al., 2019; Xu et al., 2021b; Yu et al., 2024). Wu et al. (Wu et al., 2021) have developed heat-responsive self-healing polyurethane-urea synthesized by renewable feedstocks. The healing efficiency of the polyurethance-urea system was found to be up to 94 % when they were healed at 120 °C for 10 min and the self-healing mechanism occurred from reversible crosslinking Diels–Alder reactions was reported. In addition, bio-derived vanillin-furfurylamine based benzoxazine (V-fa)/epoxidized castor oil copolymers exhibiting both self-healing and shape memory effects were prepared by Amornkitbamrung et al. (Amornkitbamrung et al., 2022). They have detailed that the copolymer could heal their crack by indirect heating from near-infrared (NIR) light for 20 min via dynamic covalent bonds incorporated by crosslinker of glutaric anhydride functionalization. Therefore, fast thermo-responsive self-healing polymer from bio-derived polymer without functionalization of crosslinker was studied and developed in this work.

Herein the influence of benzoxazine/epoxy weight ratios on thermal property, mechanical property and self-healing performance under heating stimulation displayed by the bio-derived copolymers–synthesized from bio-derived substances; eugenol-furfurylamine based benzoxazine and epoxy–was investigated. The focus of this work is to develop a novel fast thermo-responsive thermoset self-healing copolymers made entirely of bio-derived benzoxazine/epoxy copolymers. Numerical simulation technique was also utilized to predict possibility for using the self-healing copolymers as roof coatings.

2. Materials and preparation

2.1. Materials

There are two resins used in this study i.e., bio-derived benzoxazine resin—synthesized from eugenol, furfurylamine and paraformaldehyde—, and bio-derived epoxy resin namely epoxidized castor oil (ECO) — supported by Aditya Birla Chemicals Thailand Ltd., Rayong, Thailand. Eugenol (>99.0 %) and furfurylamine (98.0 %) were purchased from Tokyo Chemical Industry Co., Ltd., United States. Paraformaldehyde (AR grade) was purchased from Sigma-Aldrich Pte. Ltd., United States. All chemicals were used as received.

2.2. Benzoxaizne resin preparation

Benzoxazine resin (E-fa) was synthesized from eugenol, furfurylamine, and paraformaldehyde at a molar ratio of 1:1:2 via solventless synthesis technique (Ishida, 1996) as shown in Scheme 1 (a). The three reactants were gently stirred at 110 °C for 40–45 min to yield a homogeneous mixture. Then, the mixture was settled at room temperature and subsequently obtained the yellow resin.

2.3. Bio-derived benzoxazine/epoxy copolymer preparation

Bio-derived benzoxazine/epoxy copolymer preparation is shown in Scheme 1 (b) (Hombunma et al., 2019). The E-fa was mixed with ECO to prepare E-fa/ECO mixtures at various weight ratios (i.e., 90/10, 80/20,

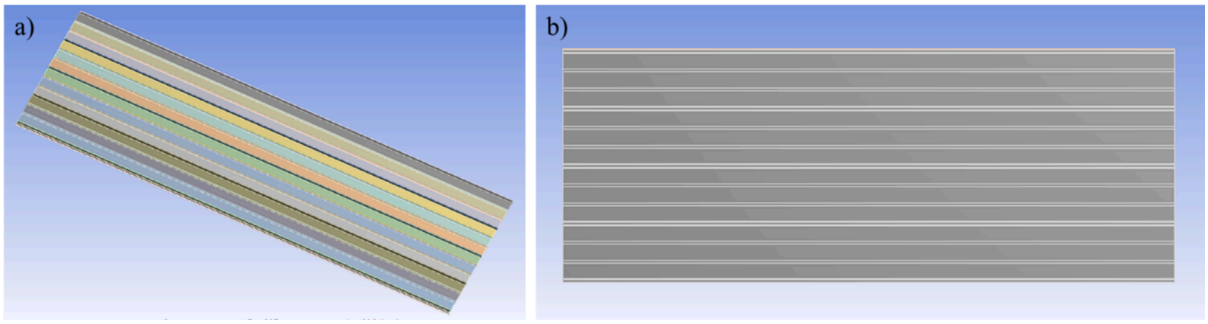

Fig. 1. The geometry of the roof coated with copolymer coating: a) side view and b) rear view.

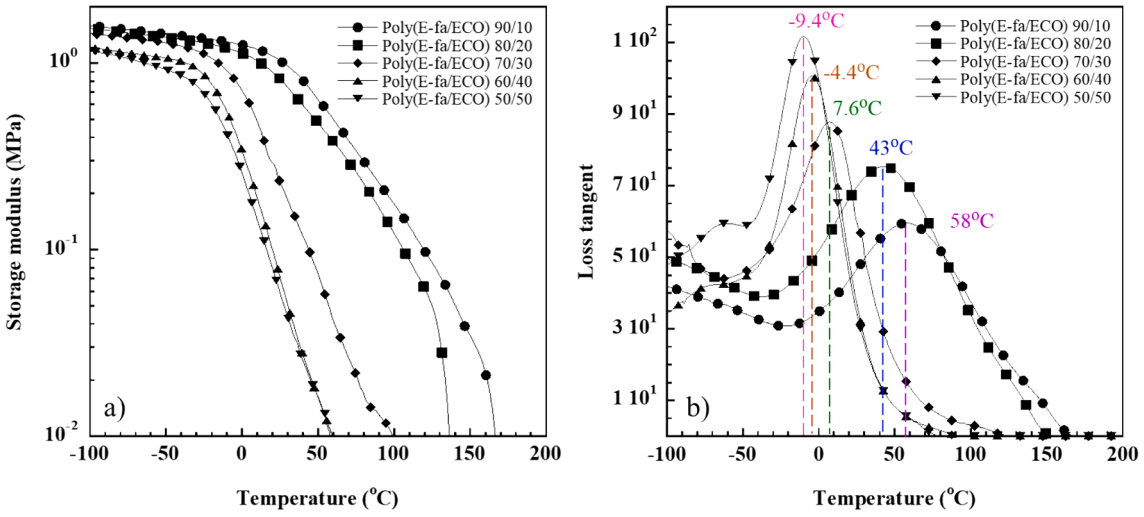

Fig. 2. Dynamic mechanical property (a) storage modulus and (b) loss tangent of E-fa/ECO copolymer at various ECO contents.

70/30, 60/40 and 50/50). The mixture was heated to 110 °C and constantly mixed to achieve a homogenous mixture. After being poured into an aluminum mold, the molten mixture was step-cured in an air-circulated oven at 150 °C and 160 °C for 1 h each followed by curing at 180 °C and 190 °C for 2 h each. The specimen was cooled down to room temperature for further characterizations.

2.4. Sample characterization

Dynamic mechanical properties of specimen were investigated using a Dynamic mechanical analyzer (DMA) (model DMA242 from NETZSCH, Inc., Bavaria Germany). The test was run in tension mode. The specimens measured 30 mm × 5 mm × 0.5 mm. At a frequency of 1 Hz, the strain at 5 μm amplitude was applied in a sinusoidal manner. Under nitrogen environment, the temperature was scanned from −100 – 200 °C with heating rate of 5 °C/min.

Differential scanning calorimetry (DSC) model DSC25 from TA Instruments Ltd was used to investigate reversible reaction of samples upon heating and cooling. An aluminum pan with a cover was used to contain a sample mass of 3–5 mg, which was then heated at a rate of 10 °C/min from 30 °C to 200 °C while nitrogen was purging at a rate of 50 ml/min.

Fourier transform infrared spectra of specimen were carried out from FTIR spectrophotometer: TENSOR 27 Bruker, Heating ATR diamond. Number of scans at 64 were used to capture the spectrum, with a spectral range of 4000–400 cm^{-1} and resolution of 4 cm^{-1}.

Tensile properties were investigated standard using Universal Testing Machine (Model LR10K) Brand LLOYD according to ASTM D3039. The dimensions of samples are 100 mm × 8 mm × 0.5 mm with a crosshead speed of 10 mm/min. Five tests were carried out for each sample.

The 90° peel strength was also studied by using Universal Testing Machine (Model LR10K) Brand LLOYD based on ASTM D6862. At least five samples with dimension of 8 mm width and 0.5 mm thick of peel test were tested and averaged at peel rate of 50 mm/min. The AISI 304 stainless steel was used as substrate backup board.

Optical micrographs in reflection modes were used to investigate surface healing behavior of samples using an Axio Scope.A1 with an AxioCam HRc CCD camera (Carl Zeiss Co., Ltd., Bangkok, Thailand).

The tensile strength and stress occurred under coating application condition of specimen were investigated by using numerical simulation. The test incident and specimen stress were numerically performed using a commercial version of ANSYS AUTODYN. The tensile test was performed on the specimen dimension with a speed test based on the experimental testing. Whereas, the copolymer-coated roof was constructed with four fixed edges under isotropic materials. The geometry of the stainless-steel roof was generated according to MasterRib Roof System having 36-inch siding and 96-inch long as shown in Fig. 1. Input coating test conditions were based on tropical storm with wind velocity of 191 mph (306 km/h) and environmental temperature of 50 °C (Ghosh & Chakravarty, 2018).

3. Results and discussion

3.1. Dynamic mechanical property of E-fa/ECO copolymers at various ECO contents

The study of thermo-mechanical characteristics of polymers is

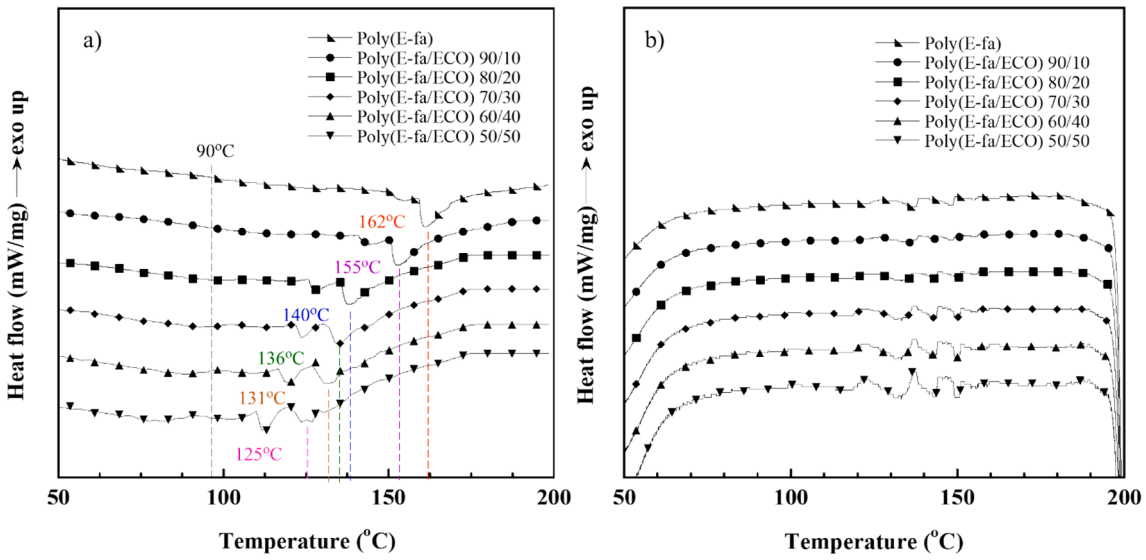

Fig. 3. DSC thermograms of E-fa/ECO copolymers at various ECO contents in (a) heating segment and (b) cooling segment.

Table 1
Heating enthalpy and cooling enthalpy of the E-fa/ECO copolymers at various ECO contents.

Sample	Heating enthalpy (J/g)	Cooling enthalpy (J/g)
Poly(E-fa)	2.20	0.127
Poly(E-fa/ECO) 90/10	2.15	0.110
Poly(E-fa/ECO) 80/20	2.06	0.088
Poly(E-fa/ECO) 70/30	1.98	0.068
Poly(E-fa/ECO) 60/40	1.89	0.046
Poly(E-fa/ECO) 50/50	1.84	0.029

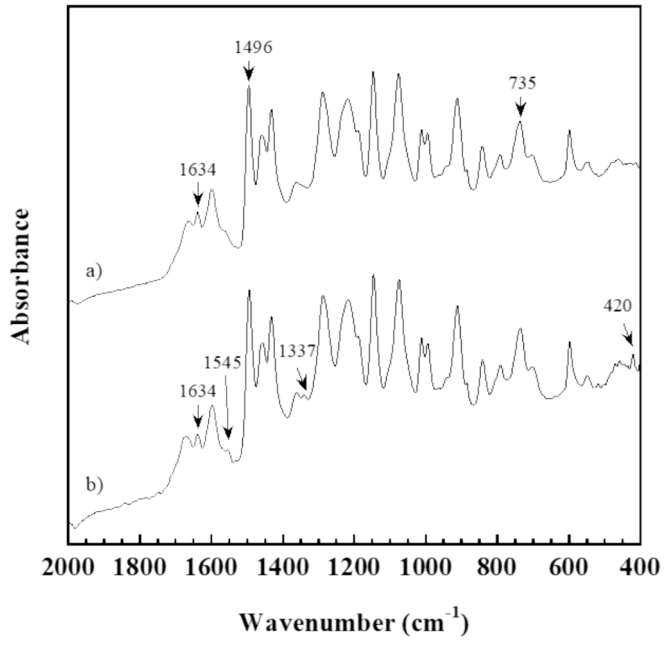

Fig. 4. FTIR spectra of E-fa/ECO copolymer at weight ratio of 50/50 wt% at a) room temperature and b) transition temperature.

commonly used dynamic mechanical analysis. Temperature-dependent storage modulus of E-fa/ECO copolymers at different ECO contents are exhibited in Fig. 2(a). The storage modulus of the copolymers at the glassy state (−100 °C) was declined from 1.59 GPa to 1.16 GPa as ECO contents increased ranging of 10–50 wt% as expected. This is due to the fact that copolymers had more flexible ECO content, which led to a more flexible polymer network (Prathumrat et al., 2017; Rimdusit et al., 2011).

Transition temperature is one of the most important factors for SHP performance, which improved by high polymer network mobility with sufficient low T_g. The T_g of E-fa/ECO copolymers at different ECO concentrations was obtained from loss tangent curves at the maximum peak as shown in Fig. 2(b). From the results, T_g of the copolymers were decreased from 58 °C to −9.4 °C when ECO was added. The decrease in T_g is possibly owning to long alkyl chains of epoxy which might be aided by a decrease in crosslink density. The T_g value of the copolymers decreased as molecular mobility increased (Hombunma et al., 2019). Moreover, the DMA results also showed that the storage modulus of all copolymers was gradually decreased after reaching T_g. This might be affected by state changing of the copolymers from rubbery state to liquid-like state (Mrlík et al., 2020).

3.2. *Self-healing effect of E-fa/ECO copolymers at various ECO contents*

The state changing of E-fa/ECO copolymers at various ECO concentrations was studied by DSC in both heating and cooling segments as shown in Fig. 3. The enthalpy of the copolymers at various ECO contents are tabulated in Table 1. From the results, the neat poly(E-fa) and all copolymers were found broad endothermic peaks in heating segment (Fig. 3(a)) and small exothermic peaks in cooling segment (Fig. 3(b)). Heating and cooling enthalpies of the copolymers were systematically decreased with decreasing the E-fa contents. This indicates that the reversible state changing generated by poly(E-fa) resulted in state transition of E-fa/ECO copolymers between rubbery state and liquid-like state. Additionally, the endothermic peaks of the copolymers, which are the maximum state changing, dropped from 162 °C to 125 °C as the ECO contents increased was observed that may thank to the flexibility of the polymer network facilitated by the long alkyl chains of ECO (Hombunma et al., 2019). However, the onset endothermic peaks of the neat poly(E-fa) and all copolymers were found as similar as at approximately 90 °C. Therefore, the results implied that reversible state changing of all E-fa/ECO copolymers could initially occur at ~ 90 °C which is one of the crucial parameters for being self-healing polymers. The similar findings of self-healing thermoplastic polyurethane (TPU) and poly(ε-caprolactone) (PCL) measured by DSC in the range of 110–150 °C were identified to be reversible reaction known as Diels-Alder reaction reported by Bi et al. (Bi et al., 2022). Furthermore, to

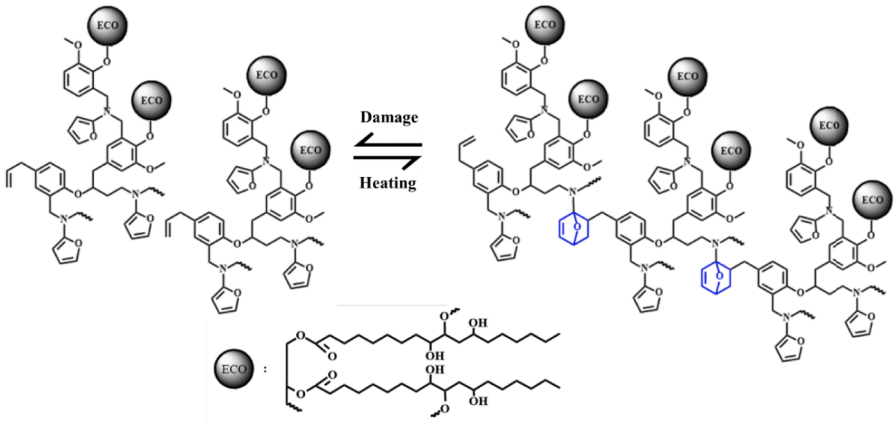

Fig. 5. A possible Diels-Alder reaction occurred in E-fa/ECO copolymers.

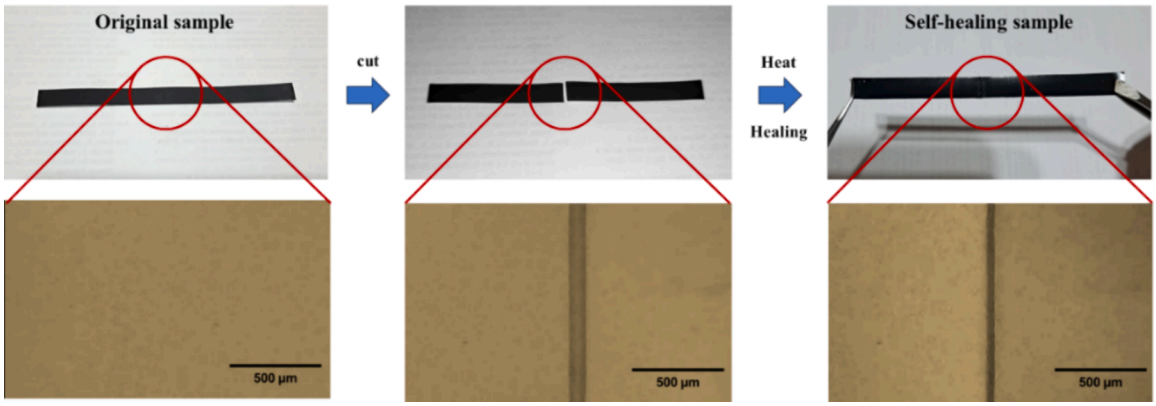

Fig. 6. Healing test of E-fa/ECO copolymers.

avoid completely deformation of the copolymers at the maximum endothermic peaks for further applications, the onset endothermic peaks at 90 °C was applied as the healing temperature in this work.

The reversible reaction of E-fa/ECO copolymer at weight ratio of 50/50 wt% between room temperature (RT) and transition temperature (~90 °C) was studied by FTIR spectroscopy with heating ATR as shown in Fig. 4. From the spectrum, the copolymer at RT demonstrated the absorption band at 1496 cm^{-1} which is the tetra-substituted arene of poly(E-fa) obtained from the ring-opening reaction of E-fa (Ishida & Sanders, 2000; Mora et al., 2021; Prasomsin et al., 2019). The characteristic peak of furan group and C=C stretching of poly(E-fa) was observed at 735 and 1634 cm^{-1}, respectively (Hombunma et al., 2019). On the other hands, the FTIR spectrum of the copolymer at transition temperature presented the new absorption bands at 420 and 1545 cm^{-1} attributed to cyclohexene group of the copolymers (Mostafalou & Mohammadi, 2024). The new absorption peak at 1337 cm^{-1} referred to 2,5 dihydrofuran group was also found in the E-fa/ECO copolymer at transition temperature (Api et al., 2023). Moreover, the decreased band at 1634 cm^{-1} suggested to C=C stretching of poly(E-fa) was observed (Hombunma et al., 2019). This is might be attributed to Diels-Alder reversible reaction between double bond (C=C) and furan group of poly(E-fa) (Wu et al., 2021) was occurred during heating beyond transition temperature. A possible Diels-Alder reaction occurred in E-fa/ECO copolymers is presented in Fig. 5. The results suggested that the self-healing behavior of E-fa/ECO copolymers occurred during state changing via the Diels-Alder reaction at transition temperature of ~ 90 °C for further investigation.

3.3. Self-healing behavior of E-fa/ECO copolymers at various ECO contents

To investigate the macroscopic self-healing behavior, a rectangular sample of E-fa/ECO copolymers was cut into two sections, and the newly exposed surfaces were brought into immediate touch (Fig. 6). It was then subjected to heating at transition temperature of 90 °C for 2 min to allow Diels–Alder reactions. The repaired sample can then be stretched without breaking. Fig. 7 shows the microscopic healing process of E-fa/ECO copolymers at various ECO contents. The surfaces of the sample were provided after healing at 90 °C for 0, 1 and 2 min. From the results, the surface of the copolymers was more healed with increasing healing time. In addition, the surface of the copolymers was less healed with increasing ECO contents. This phenomenon was explained by the decrease in E-fa contents which could generate the Diels–Alder reactions leading to lower self-healing performance.

Due to tensile strength at the service temperature of RT which plays an important role in the coating applications, the tensile strength therefore was reported and studied as the parameter change under healing process. Table 2 shows the tensile strength of E-fa/ECO copolymers at various ECO contents before and after healing. Healing performance of E-fa/ECO copolymers was calculated by Eq. (1) with comparison of the tensile strength of the specimen before and after healing by heating at transition temperature of 90 °C for 2 min.

$$\%Healing = \left(TS_{after}/TS_{before}\right) \times 100 \quad (1)$$

where TS_{after} is tensile strength of specimen after healing and TS_{before} is tensile strength of specimen before healing.

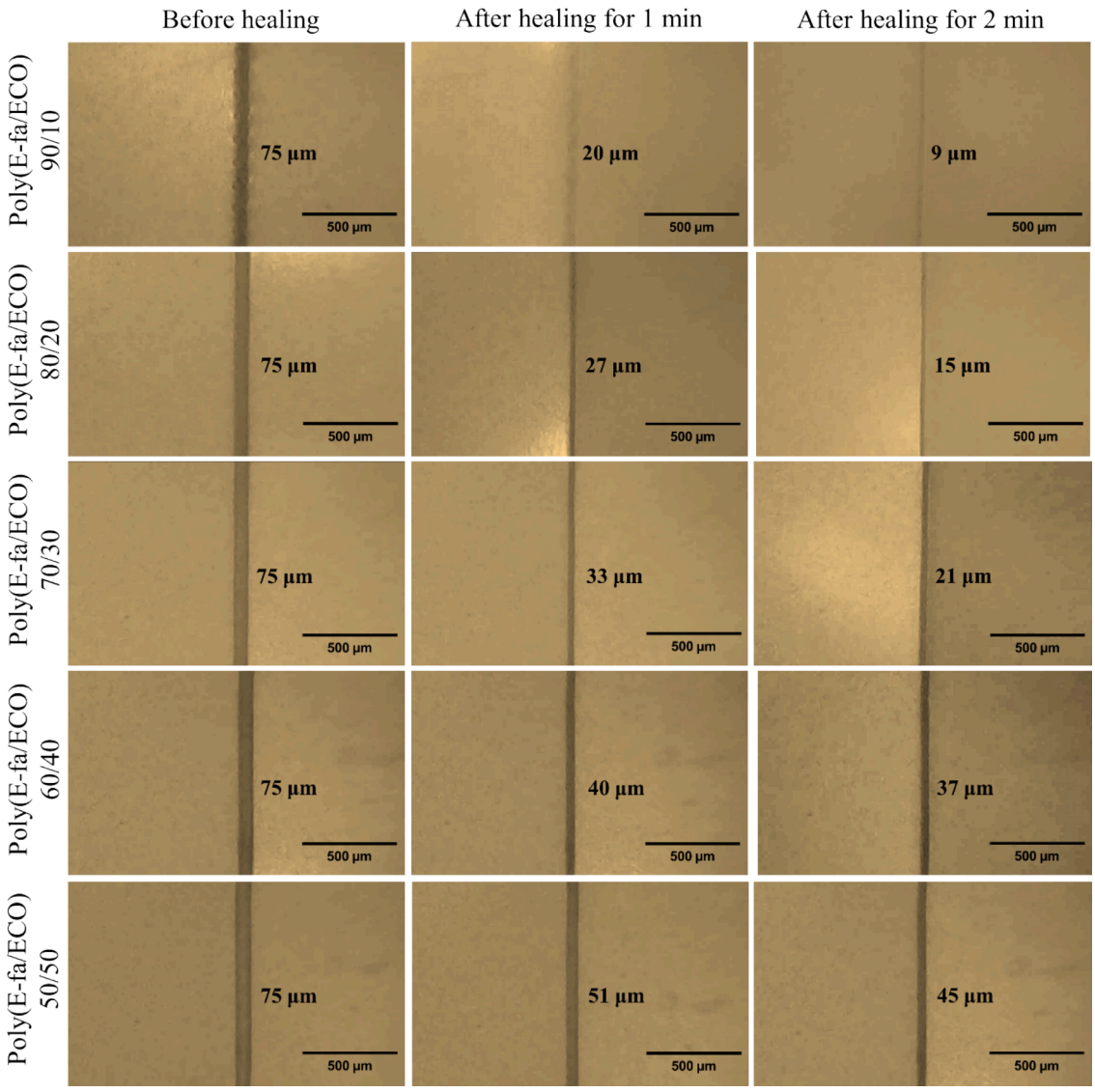

Fig. 7. Microscopic healing process of E-fa/ECO copolymers at various ECO contents.

Table 2
Healing performance and tensile strength of E-fa/ECO copolymers at various ECO contents before and after healing.

Sample	Tensile strength before healing (MPa)	Tensile strength after healing (MPa)	% Healing
Poly(E-fa/ECO) 90/10	2.17 ± 0.12	2.02 ± 0.11	93
Poly(E-fa/ECO) 80/20	2.74 ± 0.08	2.47 ± 0.07	90
Poly(E-fa/ECO) 70/30	3.68 ± 0.08	3.20 ± 0.07	87
Poly(E-fa/ECO) 60/40	2.10 ± 0.05	1.73 ± 0.04	82
Poly(E-fa/ECO) 50/50	1.74 ± 0.10	1.31 ± 0.08	75

From the results, it was discovered that adding ECO up to 30 wt% enhanced the tensile strength of the copolymers by up to 3.68 MPa. This might be attributed to the softer ECO could help to improve the flexibility of the copolymers that led to improve load transfer of the sample. Nevertheless, tensile strength dropped to 1.74 MPa when ECO was added to poly(E-fa) at a weight percentage higher than 30 % due to adequate ECO softening (Parnklang et al., 2019; Takeoka et al., 2020). From Table 2, healing performance of the copolymers was decreased with increasing epoxy content. This aligns well with the earlier findings which was due to the decrease the reversible Diels–Alder reactions in E-fa that acted as healing agents in the copolymers. Furthermore, healing performance of our developed E-fa/ECO copolymers (75–93 %) was

Table 3
Peel strength onto stainless steel substrate of E-fa/ECO copolymers at various ECO contents.

Sample	Peel strength (N/mm)
Poly(E-fa/ECO) 90/10	0.68 ± 0.02
Poly(E-fa/ECO) 80/20	0.71 ± 0.02
Poly(E-fa/ECO) 70/30	0.75 ± 0.01
Poly(E-fa/ECO) 60/40	0.80 ± 0.01
Poly(E-fa/ECO) 50/50	0.84 ± 0.01

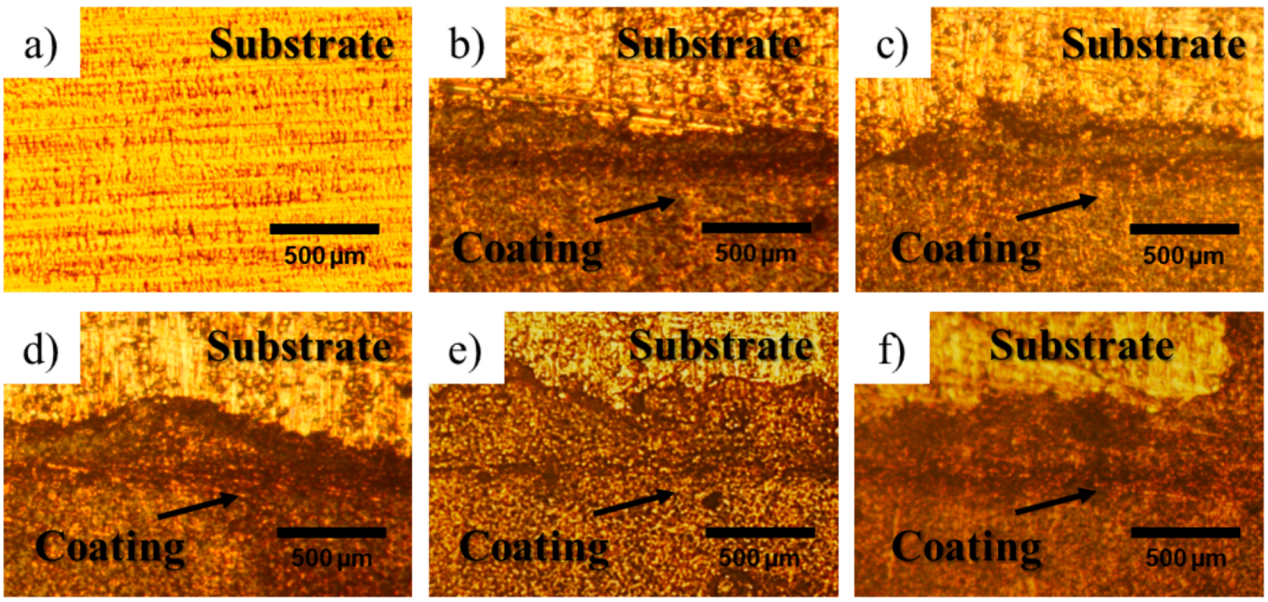

Fig. 8. Failure surface after peeling test of E-fa/ECO copolymers at various ECO contents: a) stainless steel, b) 10 wt%, c) 20 wt%, d) 30 wt%, e) 40 wt% and f) 50 wt%.

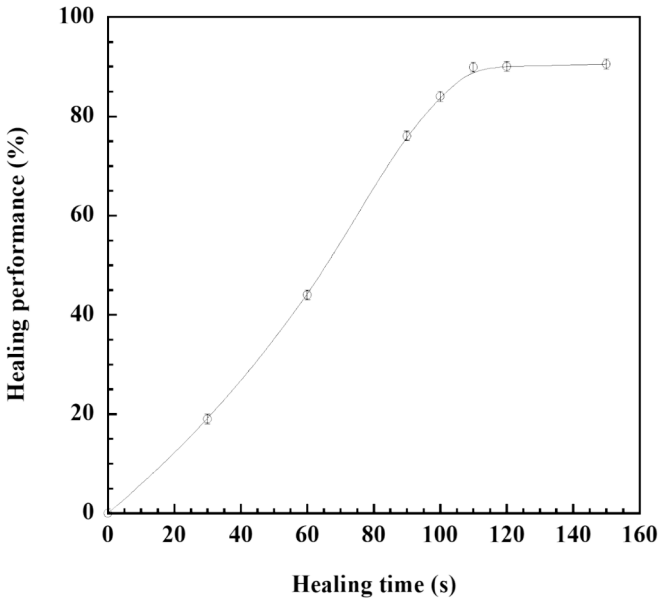

Fig. 9. Healing performance of E-fa/ECO copolymer at different healing times.

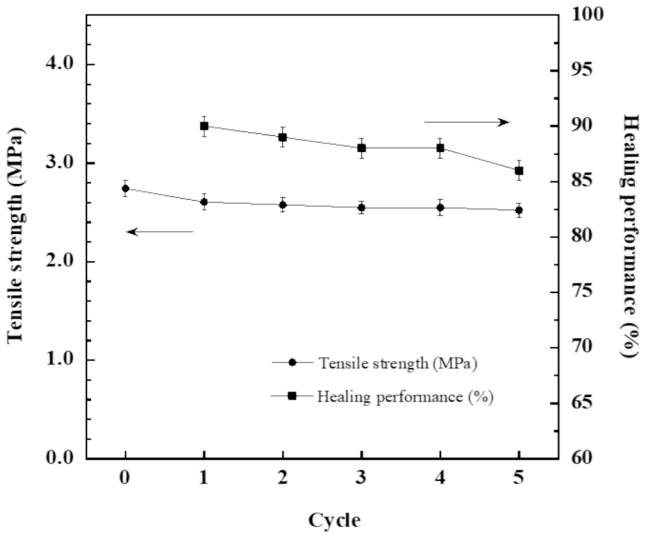

Fig. 10. Tensile strength after healing and healing performance of E-fa/ECO copolymer at ECO content of 20 wt% versus healing cycle.

higher than that of multistimuli-responsive intrinsic self-healing epoxy resin produced through host–guest interactions (~79.2 %) (Hu et al., 2018) and methacrylic acid (MAAc) and poly(ethylene glycol) methyl ether methacrylate (OEGMA) random copolymer: poly(MAAc-*co*-OEGMA) (~60–80 %) (Diggle et al., 2021).

3.4. Peel strength of self-healing materials based on E-fa/ECO copolymers at various ECO contents

The adhesion to the substrate is one of the most important properties of the coatings which was indicated to the strong bond between them and substrate (George et al., 2023). Peel strength onto stainless steel substrate of self-healing materials based on E-fa/ECO copolymers at various ECO contents was studied as shown in Table 3. The peel strength for the copolymers increased with growth in ECO contents. The strength of the copolymers increases with increase in ECO content reflects the increases the interfacial strength which might be occurred by intermolecular bonds of H-bond between hydroxyl group of stainless steel surface and E-fa/ECO copolymers (Schmidt & Bell, 1986; Wei et al., 2020). The addition of ECO into the copolymers could enhance the amount of hydroxyl group of E-fa/ECO copolymers from opening oxirane ring of epoxy and oxazine ring of benzoxazine resin after thermal curing as provided a possible structure in Scheme 1(b) which substantially improve peel strength of the copolymers (Hombunma et al., 2019). Moreover, the adhesion mechanism of the developed copolymers after peeling test was also investigated by optical microscope as shown in Fig. 8. From the results, the surfaces of all copolymers were found some layer of the copolymers remaining on the substrate surface. This indicated that the adhesion mechanism of E-fa/ECO copolymers onto stainless steel was the cohesive failure representing sufficient adhesion strength between the coating and substrate (Ebnesajjad, 2014). Moreover, the peel strength of our developed copolymers was in the similar range of that of commercial epoxy coating of 0.70 N/mm tested with the same conditions. The results suggested that the adhesion to stainless steel substrate of the copolymers were substantially improved with the

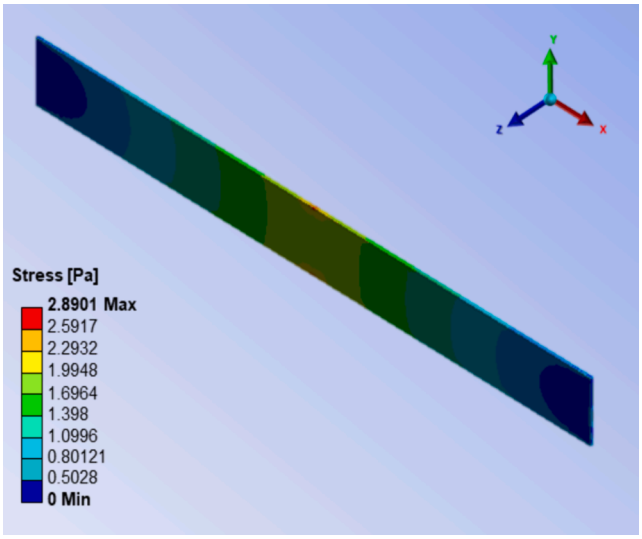

Fig. 11. Numerical stress of E-fa/ECO copolymer at 20 wt% of ECO under tension mode.

incorporation of ECO at 20 wt% or higher and sufficient for stainless steel coating applications.

3.5. Repeated healing cycles of self-healing material based on E-fa/ECO copolymer

According to our earlier findings, E-fa/ECO copolymer with ECO content of 20 wt% offered good self-healing ability of 90 % combined with a superior assortment of thermomechanical properties (T_g of 43 °C which higher than service temperature at RT of 25 °C and storage modulus of 1.53 MPa) and mechanical property (tensile strength of 2.74 MPa and peel strength onto stainless steel substrate of 0.71 N/mm). Consequently, as shown in Fig. 9, the SHP sample based on E-fa/ECO copolymer was studied the effect of healing time on healing performance. The results showed that the healing performance was increased up to 90 % with increasing healing time up to approximately 112 s. In addition, healing performance of our developed E-fa/ECO copolymers was in the similar range of healing efficiency with faster healing time when compared to those of the polyurethance-urea system (healing efficiency of 94 % with thermo-responsive healing time for 10 min) (Wu et al., 2021) and bio-derived V-fa/ECO copolymers (healing efficiency of 93 % with healing time for 20 min) (Amornkitbamrung et al., 2022). From the results, SHP based on E-fa/ECO copolymer at ECO content of 20 wt% with healing time of 112 s was subjected to further analysis of healing cycles. Furthermore, the impact of healing cycles on tensile strength after healing and its healing performance was evaluated and illustrated in Fig. 10. It was observed that there was no discernible difference in healing capability up to five cycles, suggesting that the self-healing ability of the copolymer was remarkably stable.

3.6. Numerical simulation analyses of roof coatings based on E-fa/ECO copolymer

Numerical simulation was initially performed to assess the suitability of input property of E-fa/ECO copolymer at 20 wt% of ECO by comparing tensile strength from experimentation and simulation. The simulated tensile strength of the copolymer is illustrated in Fig. 11.

Table 4
Isotropic material properties of stainless-steel roof and E-fa/ECO copolymer.

Properties	Stainless steel roof	Coating based on E-fa/ECO copolymer at 80/20 wt%
Thickness (mm)	8	0.5
Density (g/cm^3)	7.850	1.128
Young modulus (Pa)	2.0×10^{11}	8.1×10^{8}
Poisson's ratio	0.3	0.45
Bulk modulus (Pa)	1.67×10^{11}	2.71×10^{9}
Shear modulus (Pa)	7.7×10^{10}	2.803×10^{8}

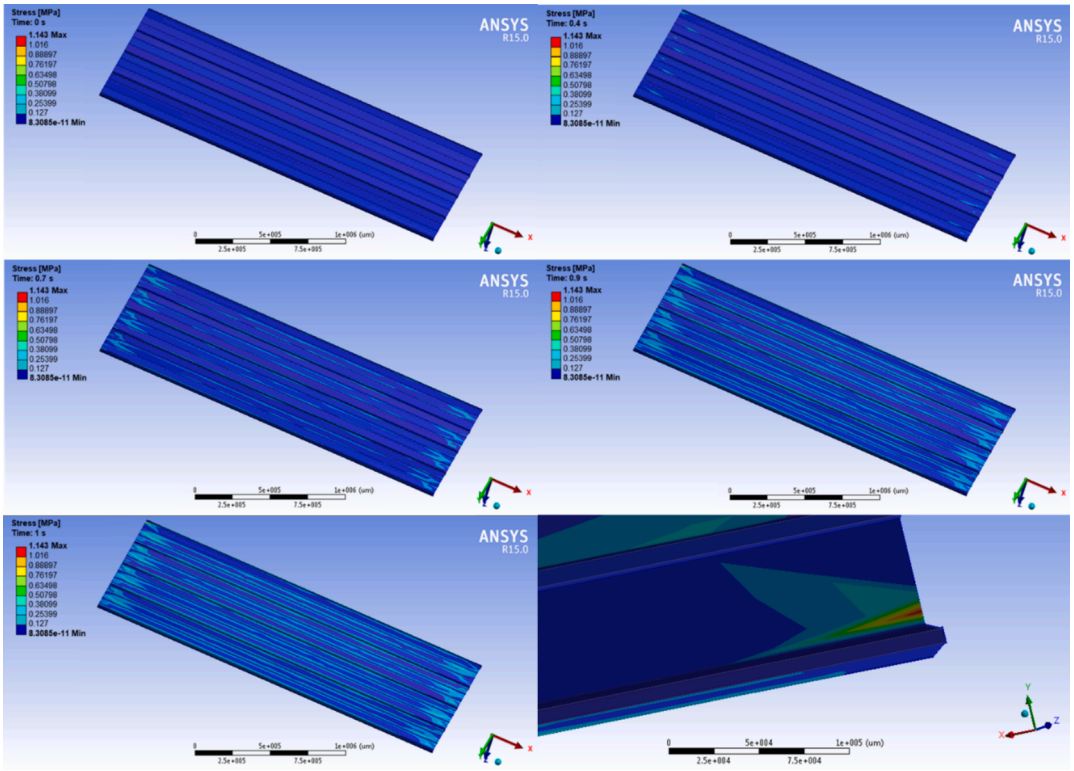

Fig. 12. Numerical simulation analyses performed on E-fa/ECO copolymer undergoing wind impact.

Based on the data, it was estimated that numerical tensile strength of the copolymer would be 2.89 MPa, 5 % difference from the previously stated experimental tensile strength of 2.74 MPa. Likewise, there was a qualitative similarity between the simulated and experimental tensile strength values. Therefore, the input property of E-fa/ECO copolymer at 20 wt% of ECO was applied in further the roof coating study.

To study the performance of SHP based on E-fa/ECO copolymer in roof coating application under tropical storm condition with wind velocity of 191 mph (306 km/h) and environmental temperature of 50 °C, numerical simulation was utilized to study the response of the specimen as shown in Fig. 12. The isotropic material properties of stainless-steel roof and E-fa/ECO copolymer at 20 wt% of ECO specimen are presented in Table 4. The results were found that the stress occurred as the wind impact time on the roof. After impact incident, the maximum stress was growth on the E-fa/ECO coating layer at the edge without damaging stainless steel roof with the value of 1.143 MPa which is lower than the strength of the copolymer. The results revealed that the damage occurred on the coating layer which could be healed by fast thermo-responsive self-healing effect at 90 °C for 112 s to protect the structural roof suggesting possibility for coating application.

4. Conclusions

This work has been successfully developed thermo-responsive thermoset self-healing polymers based on bio-derived E-fa/ECO copolymers. The effect of ECO contents at 10–50 wt% on thermal property, mechanical property and self-healing performance of the copolymers was investigated. The outcomes of DSC and FTIR results indicated the reversible Diels-Alder reaction was formed in the copolymers structure triggered by heating. Healing temperature of E-fa/ECO copolymers was initially occurred at approximately 90 °C with the addition of ECO contents up to 50 wt%. The mechanical property under tension mode and peel strength to stainless steel were also substantially enhanced with the incorporation of ECO. In term of SHP performance, healing performance was enhanced with increasing E-fa contents. The results revealed that the healing performance of the copolymers was substantially improved up to 93 % with increasing healing time at less than approximately 2 min. Furthermore, the numerical results predicted that stress under tropical storm of roof coated with E-fa/ECO copolymers was occurred on the coating layer. The results suggested that the bio-derived benzoxazine/epoxy copolymers have a potential use in SHP coating materials with reverse healing more than 5 cycles.

Funding

This work receives financial supports from the NSRF via the Program Management Unit for Human Resources and Institutional Development, Research and Innovation (grant number B05F640094), Faculty of Engineering, Srinakharinwirot University (grant number 196/2023), the National Research Council of Thailand (NRCT) and Srinakharinwirot University (grant number N42A650377), University Development Fund (grant number: 588/2565), and National Research Council of Thailand (NRCT) and Chulalongkorn University (grant number N42A660910).

CRediT authorship contribution statement

Phattarin Mora: Writing – review & editing, Writing – original draft, Visualization, Methodology, Funding acquisition, Conceptualization. **Sarawut Rimdusit:** Funding acquisition. **Chanchira Jubsilp:** Writing – review & editing, Supervision, Funding acquisition.

Declaration of Competing Interest

The authors declare that they have no known competing financial interests or personal relationships that could have appeared to influence the work reported in this paper.

References

Amaral, A.J.R., Pasparakis, G., 2017. Stimuli responsive self-healing polymers: gels, elastomers and membranes. Polym. Chem. 8, 6464–6484. https://doi.org/10.1002/pen.26939.

Amornkitbamrung, L., Leungpuangkaew, S., Panklang, T., Jubsilp, C., Ekgasit, S., Um, S. H., Rimdusit, S., 2022. Effects of glutaric anhydride functionalization on filler-free benzoxazine/epoxy copolymers with shape memory and self-healing properties under near-infrared light actuation. J. Sci.-Adv. Mater Dev. 7(3), 100446. doi: 10.1016/j.jsamd.2022.100446.

An, S., Lee, M.W., Yarin, A.L., Yoon, S.S., 2018. A review on corrosion-protective extrinsic self-healing: Comparison of microcapsule-based systems and those based on core-shell vascular networks. Chem. Eng. J. 344, 206–220. https://doi.org/10.1016/j.cej.2018.03.040.

Api, A.M., Belsito, D., Botelho, D., Bruze, M., Burton, G.A., Cancellieri, M.A., Chon, H., Dagli, M.L., Dekant, W., Deodhar, C., Fryer, A.D., Jones, L., Joshi, K., Kumar, M., Lapczynski, A., Lavelle, M., Lee, I., Liebler, D.C., Moustakas, H., Muldoon, J., Penning, T.M., Ritacco, G., Romine, J., Sadekar, N., Schultz, T.W., Selechnik, D., Siddiqi, F., Sipes, I.G., Sullivan, G., Thakkar, Y., Tokura, Y., 2023. RIFM fragrance ingredient safety assessment, 4,5-dimethyl-3-hydroxy-2,5-dihydrofuran-2-one, CAS Registry Number 28664–35-9. Food Chem. Toxicol. 182, 114139. https://doi.org/10.1016/j.fct.2023.114139.

Arslan, M., Kiskan, B., Yagci, Y., 2015. Benzoxazine-based thermosets with autonomous self-healing ability. Macromolecules 48 (5), 1329–1334. https://doi.org/10.1021/ma5025126.

Arslan, M., Kiskan, B., Yagci, Y., 2018a. Benzoxazine-based thermoset with autonomous self-healing and shape recovery. Macromolecules 51 (24), 10095–10103. https://doi.org/10.1021/acs.macromol.8b02137.

Arslan, M., Motallebzadeh, A., Kiskan, B., Demirel, A.L., Kumbaraci, I.V., Yagci, Y., 2018b. Combining benzoxazine and ketene chemistries for self-healing of high performance thermoset surfaces. Polym. Chem. 9 (15), 2031–2039. https://doi.org/10.1039/c8py00293b.

Bi, H., Ye, G., Sun, H., Ren, Z., Gu, T., Xu, M., 2022. Mechanically robust, shape memory, self-healing and 3D printable thermoreversible cross-linked polymer composites toward conductive and biomimetic skin devices applications. Addit. Manuf. 49, 102487. https://doi.org/10.1016/j.addma.2021.102487.

Chao, A., Negulescu, I., Zhang, D., 2016. Dynamic covalent polymer networks based on degenerative imine bond exchange: tuning the malleability and self-Healing properties by solvent. Macromolecules 49 (17), 6277–6284. https://doi.org/10.1021/acs.macromol.6b01443.

Diggle, B., Jiang, Z., Li, R.W., Connal, L.A., 2021. Self-healing polymer network with high strength, tunable properties, and biocompatibility. Chem. Mater. 33 (10), 3712–3720. https://doi.org/10.1021/acs.chemmater.1c00707.

Ebnesajjad, S., 2014. Chapter 5 - Theories of Adhesion. In: Ebnesajjad, S. (Ed.), Surface Treatment of Materials for Adhesive Bonding (second Edition). Publishing. Oxford, William Andrew, pp. 77–91.

Fadl, A.M., Sadeek, S.A., Magdy, L., Abdou, M.I., El-Shiwiniy, W.H., 2021. Multi-functional epoxy composite coating incorporating mixed Cu(II) and Zr(IV) complexes of metformin and 2,2\-bipyridine as intensive network cross-linkers exhibiting anti-corrosion, self-healing and chemical-resistance performances for steel petroleum platforms. Arab. J. Chem. 14 (10), 103367. https://doi.org/10.1016/j.arabjc.2021.103367.

Fang, L., Fang, T., Liu, X., Ni, Y., Lu, C., Xu, Z., 2017. Precise stimulation of near-infrared light responsive shape-memory polymer composites using upconversion particles with photothermal capability. Compos. Sci. Technol. 152, 190–197. https://doi.org/10.1016/j.compscitech.2017.09.021.

Gao, Y.Y., Han, B., Zhao, W.Y., Ma, Z.C., Yu, Y.S., Sun, H.B., 2019. Light-Responsive Actuators Based on Graphene. Front. Chem. 7, 506. https://doi.org/10.3389/fchem.2019.00506.

George, J.S., P R, S., Thomas, S., Vijayan P, P., 2023. Chapter 13 - Mechanical properties of nanoscale polymer coatings. in: Polymer-Based Nanoscale Materials for Surface Coatings, (Eds.) S. Thomas, J.S. George, Elsevier, pp. 259-274.

Ghosh, I., Chakravarty, N., 2018. Tropical cyclone: expressions for velocity components and stability parameter. Nat. Hazards. 94, 1293–1304. https://doi.org/10.1007/s11069-018-3477-7.

Hombunma, P., Parnklang, T., Mora, P., Jubsilp, C., Rimdusit, S., 2019. Shape memory polymers from bio-based benzoxazine/epoxidized natural oil copolymers. Smart Mater. Struct. 29 (1), 015036. https://doi.org/10.1088/1361-665x/ab49e5.

Hu, Z., Zhang, D., Lu, F., Yuan, W., Xu, X., Zhang, Q., Liu, H., Shao, Q., Guo, Z., Huang, Y., 2018. Multistimuli-responsive intrinsic self-healing epoxy resin constructed by host–guest interactions. Macromolecules 51 (14), 5294–5303. https://doi.org/10.1021/acs.macromol.8b01124.

Huang, W.M., Yang, B., An, L., Li, C., Chan, Y.S., 2005. Water-driven programmable polyurethane shape memory polymer: demonstration and mechanism. Appl. Phys. Lett. 86 (11), 114105. https://doi.org/10.1063/1.1880448.

Imato, K., Nishihara, M., Kanehara, T., Amamoto, Y., Takahara, A., Otsuka, H., 2012. Self-Healing of chemical gels cross-linked by diarylbibenzofuranone-based trigger-free dynamic covalent bonds at room temperature. Angew. Chem. Int. Ed. 51 (5), 1138–1142. https://doi.org/10.1002/anie.201104069.

Ishida, H., Agag, T., 2011. Handbook of benzoxazine resins. Elsevier, Amsterdam, The Netherlands.

Ishida, H., Sanders, D.P., 2000. Regioselectivity and network structure of difunctional alkyl-substituted aromatic amine-based polybenzoxazines. Macromolecules 33 (22), 8149–8157. https://doi.org/10.1021/ma991836t.

Ishida, H. 1996. Process for preparation of benzoxazine compounds in solventless systems, US patent no. 5543516.

Ji, S., Cao, W., Yu, Y., Xu, H., 2015. Visible-light-induced self-healing diselenide-containing polyurethane elastomer. Adv. Mater. 27 (47), 7740–7745. https://doi.org/10.1002/adma.201503661.

Leungpuangkaew, S., Amornkitbamrung, L., Phetnoi, N., Sapcharoenkun, C., Jubsilp, C., Ekgasit, S., Rimdusit, S., 2023. Magnetic- and light-responsive shape memory polymer nanocomposites from bio-based benzoxazine resin and iron oxide nanoparticles. Adv. Ind. Eng. Polym. Res. 6 (3), 215–225. https://doi.org/10.1016/j.aiepr.2023.01.003.

Liu, T., Liu, L., Yu, M., Li, Q., Zeng, C., Lan, X., Liu, Y., Leng, J., 2018. Integrative hinge based on shape memory polymer composites: Material, design, properties and application. Compos. Struct. 206, 164–176. https://doi.org/10.1016/j.compstruct.2018.08.041.

Mora, P., Jubsilp, C., Bielawski, C.W., Rimdusit, S., 2021. Impact response of aramid fabric-reinforced polybenzoxazine/urethane composites containing multiwalled carbon nanotubes used as support panel in hard armor. Polymers 13 (16), 2779. https://doi.org/10.3390/polym13162779.

Mora, P., Jubsilp, C., Ahn, C.-H., Rimdusit, S., 2023. Two-way thermo-responsive thermoset shape memory polymer based on benzoxazine/urethane alloys using as self-folding structures. Adv. Ind. Eng. Polym. Res. 6 (1), 13–23. https://doi.org/10.1016/j.aiepr.2022.09.001.

Mostafalou, S., Mohammadi, P., 2024. Cyclohexene. In: Wexler, P.J. (Ed.), Encyclopedia of Toxicology (fourth Edition). Academic, Press. Oxford, pp. 405–410.

Mrlík, M., Špírek, M., Al-Khori, J., Ahmad, A.A., Mosnaček, J., AlMaadeed, M.A., Kasák, P., 2020. Mussel-mimicking sulfobetaine-based copolymer with metal tunable gelation, self-healing and antibacterial capability. Arab. J. Chem. 13 (1), 193–204. https://doi.org/10.1016/j.arabjc.2017.03.009.

Oie, H., Mori, A., Sudo, A., Endo, T., 2013. Polyaddition of bifunctional 1,3-benzoxazine and 2-methylresorcinol. J. Polym. Sci. A Polym. Chem. 51 (18), 3867–3872. https://doi.org/10.1002/pola.26784.

Parnklang, T., Boonyanuwat, K., Mora, P., Ekgasit, S., Rimdusit, S., 2019. Form-stable benzoxazine-urethane alloys for thermally reversible light scattering materials. Express Polym. Lett. 13, 65–83. https://doi.org/10.3144/expresspolymlett.2019.7.

Prasomsin, W., Parnklang, T., Sapcharoenkun, C., Tiptipakorn, S., Rimdusit, S., 2019. Multiwalled carbon nanotube reinforced bio-based benzoxazine/epoxy composites with NIR-laser stimulated shape memory wffects. Nanomaterials 9, 881. https://doi.org/10.3390/nano9060881.

Prathumrat, P., Tiptipakorn, S., Rimdusit, S., 2017. Multiple-shape memory polymers from benzoxazine–urethane copolymers. Smart Mater. Struct. 26 (6), 065025. https://doi.org/10.1088/1361-665X/aa6d47.

Rahman, M.W., Shefa, N.R., 2021. Minireview on self-healing polymers: versatility, application, and prospects. Adv. Polym. Technol. 2021, 7848088. https://doi.org/10.1155/2021/7848088.

Rimdusit, S., Bangsen, W., Kasemsiri, P., 2011. Chemorheology and thermomechanical characteristics of benzoxazine-urethane copolymers. J. Appl. Polym. Sci. 121 (6), 3669–3678. https://doi.org/10.1002/app.34170.

Rimdusit, S., Jubsilp, C., Tiptipakorn, S., 2013. Alloys and Composites of Polybenzoxazines: Properties and Applications. Springer, New York.

Schmidt, R., Bell, J., 1986. Epoxy adhesion to metals. Adv. Polym. Sci. 75, 33–71. https://doi.org/10.1007/BFb0017914.

Takeoka, Y., Liu, S., Asai, F., 2020. Improvement of mechanical properties of elastic materials by chemical methods. Sci. Technol. Adv. Mater. 21 (1), 817–832. https://doi.org/10.1080/1468696.2020.1849931.

Wei, H., Xia, J., Zhou, W., Zhou, L., Hussain, G., Li, Q., Ostrikov, K., 2020. Adhesion and cohesion of epoxy-based industrial composite coatings. Compos. Part B-Eng. 193, 108035. https://doi.org/10.1016/j.compositesb.2020.108035.

Wu, P., Cheng, H., Wang, X., Shi, R., Zhang, C., Arai, M., Zhao, F., 2021. A self-healing and recyclable polyurethane-urea Diels-Alder adduct synthesized from carbon dioxide and furfuryl amine. Green Chem. 23 (1), 552–560. https://doi.org/10.1039/D0GC03695A.

Xu, J., Chen, J., Zhang, Y., Liu, T., Fu, J., 2021a. A fast room-temperature self-healing glassy polyurethane. Angew. Chem. Int. Ed. Engl. 60 (14), 7947–7955. https://doi.org/10.1002/anie.202017303.

Xu, J., Liu, T., Zhang, Y., Zhang, Y., Wu, K., Lei, C., Fu, Q., Fu, J., 2021b. Dragonfly wing-inspired architecture makes a stiff yet tough healable material. Matter 4 (7), 2474–2489. https://doi.org/10.1016/j.matt.2021.05.001.

Yang, Y., Urban, M.W., 2013. Self-healing polymeric materials. Chem. Soc. Rev. 42 (17), 7446–7467. https://doi.org/10.1039/C3CS60109A.

Ying, Y., Liu, Z., Fan, J., Wei, N., Guo, X., Wu, Y., Wen, Y., Yang, H., 2020. Micelles-based self-healing coating for improved protection of metal. Arab. J. Chem. 13 (1), 3137–3148. https://doi.org/10.1016/j.arabjc.2018.09.005.

Yu, C., Choi, J., Lee, J., Lim, S., Park, Y., Jo, S.M., Ahn, J., Kim, S.Y., Chang, T., Boyer, C., Kwon, M.S., 2024. Functional thermoplastic polyurethane elastomers with α, ω-hydroxyl end-functionalized polyacrylates. Adv. Mater. 2403048. https://doi.org/10.1002/adma.202403048.

Zhao, X., Duan, X., Mao, X., Cao, W., Hu, H., Zhou, P., Luo, J., Xie, T., Gao, W., Li, Z., 2024. CDs microcapsules polyurethane film with improved light environment, self-healing and high strength for plant greenhouses to promote plant growth. Arab. J. Chem. 17 (1), 105451. https://doi.org/10.1016/j.arabjc.2023.105451.